FREQUENCY-DOMAIN QRM-MLD BLOCK SIGNAL DETECTION FOR SINGLE-CARRIER MULTI-USER MIMO UPLINK

Masashi Itagaki, Kazuki Takeda, Fumiyuki Adachi

Dept. of Electrical and Communication Engineering, Graduate School of Engineering, Tohoku University,
6-6-05 Aza-Aoba, Aramaki, Aoba-ku, Sendai, 980-8579 Japan
{masashi, kazuki}@mobile.ecei.tohoku.ac.jp, adachi@ecei.tohoku.ac.jp

Abstract

Multi-user multi-input multi-output (multi-user MIMO) can increase the number of users simultaneously accessing the same base station (BS) without increasing the signal bandwidth. MIMO signal detection which can provide better bit error rate (BER) performance than linear detection with less computational complexity is indispensable in order to enhance the uplink cellular capacity of multi-user MIMO. Maximum likelihood detection (MLD) employing QR decomposition and M algorithm (QRM-MLD) is one of its candidates. It can reduce the complexity of MLD drastically and obtain BER performance close to MLD. QRM-MLD has been widely studied for MIMO spatial multiplexing using orthogonal frequency division multiplexing (OFDM). Recently, it has been reported that QRM-MLD can be applied to the signal detection of single-carrier (SC) transmission in a frequency selective fading channel. In this paper, we introduce the frequency-domain QRM-MLD block signal detection to the SC multi-user MIMO uplink of a cellular system and evaluate the uplink capacity. We show that QRM-MLD can obtain larger uplink cellular capacity compared to the minimum mean square error detection (MMSED) at the cost of the increased computational complexity, but with much less than MLD.

Keywords: Multi-user MIMO; single-carrier ; QRM-MLD; uplink capacity

1 Introduction

Multi-user multi-input multi-output (MIMO) [1], [2] can provide multiple users with high speed data services without increasing the signal bandwidth. For uplink single-carrier (SC) multi-user MIMO in a cellular system, the signal detection at the base station (BS) is quite complex due to the strong interference, such as inter-symbol interference (ISI), multi-user interference (MUI), and co-channel interference (CCI). Severe ISI is produced due to the strong channel selectivity [3]. In multi-user MIMO, multiple users transmit their data to the same BS using the same carrier frequency and this produces the MUI. Furthermore, in cellular systems, the same carrier frequency is reused at spatially separated different cells in order to efficiently utilize the limited frequency bandwidth [4] and therefore, the CCI is produced.

The uplink cellular capacity of SC multi-user MIMO with zero-forcing detection (ZFD) and minimum mean square error detection (MMSED) in a frequency selective fading channel was discussed in [5]. Although ZFD and MMSED are computationally efficient, the achievable uplink capacity is much smaller than that of maximum likelihood detection (MLD). MLD requires prohibitively high complexity. MLD employing QR decomposition and M algorithm (QRM-MLD) [6] achieves near MLD performance with reduced complexity.

QRM-MLD has been widely studied for MIMO spatial multiplexing using orthogonal frequency division multiplexing (OFDM) [6], [7]. Recently, the frequency domain block signal detection using QRM-MLD was proposed for the SC transmission in a frequency selective fading channel [8]. QRM-MLD can be applied to the broadband SC multi-user MIMO. In this paper, we introduce frequency domain QRM-MLD block signal detection to the broadband SC multi-user MIMO uplink of a cellular system and examine how it can enhance the uplink capacity compared to MMSED.

The rest of this paper is organized as follows. Sect. 2 gives the CCI model. Sect. 3 presents the SC multi-user MIMO uplink model. In Sect. 4, frequency-domain QRM-MLD block signal detection for the SC multi-user MIMO is described. The cellular capacity achievable by the multi-user MIMO using frequency-domain QRM-MLD block signal detection is discussed in Sect. 5. Sect. 6 offers the conclusion.

2 CCI model

Figure1 illustrates the CCI model for the SC multi-user MIMO uplink in a cellular system. *U* users are simultaneously transmitting their data to the same

978-1-4244-6853-9/10/$26.00 ©2010 IEEE

BS using the same carrier frequency. It is assumed that the BS has N_r ($\geq U$) receive antennas while each user has a single transmit antenna.

In a cellular system, the whole channels are divided into a number of channel groups and each channel group is allocated to a different cell [4]. The number of different channel groups is defined as the cluster size N. As smaller N is used (the co-channel cells get closer), the number of channels per cell can be increased, but the CCI gets stronger. Therefore, there exists the optimum N that maximizes the cellular capacity. We consider 6 nearest co-channel cells since their CCIs limit the cellular capacity. The cell of interest is indexed as c=0, and 6 nearest co-channel cells are indexed as c=1~6 (see Fig. 1).

In this paper, we measure the distribution of local average bit error rate (BER) by the Monte-Carlo numerical method to find the outage probability, which is defined as the probability of the local average BER exceeding the required BER. We define the uplink capacity as the maximum number $U_{\max}$ of supportable users normalized by the cluster size N for the given allowable outage probability Q.

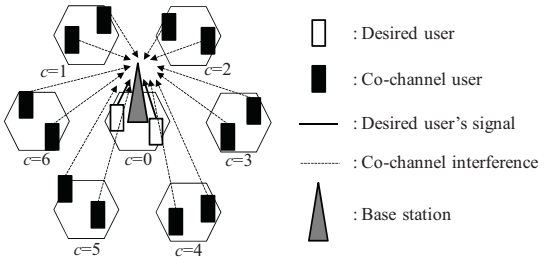

Figure 1 CCI model of SC multi-user MIMO uplink in a cellular system.

3 SC Multi-user MIMO

Figure 2 illustrates the SC multi-user MIMO uplink transmission system model. At a mobile transmitter, each user's binary data sequence is data-modulated and divided into a sequence of blocks of N_c symbols each. The last N_g symbols in each block are copied and inserted as a cyclic prefix (CP) into the guard interval (GI) to form a block of N_g+N_c symbols. Without loss of generality, the transmission of one block is considered, and the transmit timing offset plus maximum propagation time delay among U users of the cell of interest is assumed less than the GI length.

The transmitted signal block is assumed to go through a frequency-selective fading channel which is composed of L distinct paths. The channel impulse response between the u-th user in the c-th cell and the m-th receive antenna of the c=0th cell BS is given by

$$h_{m,u(c)}(\tau)=\sum_{l=0}^{L-1}h_{m,u(c)}^{(l)}\cdot\delta\left(\tau-\tau_{u(c),l}\right), \tag{1}$$

where

$$h_{m,u(c)}^{(l)}=\sqrt{r_{u(c)}^{-\alpha}\cdot 10^{-\eta_{u(c)}/10}}\cdot g_{m,u(c)}^{(l)} \tag{2}$$

with $r_{u(c)}$, $\eta_{u(c)}$, and α denoting the distance between the user and the c=0th BS, the shadowing loss, and the path-loss exponent, respectively, and $g_{m,u(c)}^{(l)}$ and $\tau_{u(c),l}$ being the complex-valued path gain and time delay of the l-th path of the u-th user in the c-th cell, respectively, with $E\left[\sum_{l=0}^{L-1}\left|g_{m,u(c)}^{(l)}\right|^2\right]=1$.

At BS of the c=0th cell, the superposition of U user's transmitted signals and CCI is received by N_r receive antennas. The GI-removed received signal block at m-th antenna $\mathbf{y}_m=\left[y_m(0)\ \cdots\ y_m(N_c-1)\right]^T$ can be expressed as [9]

$$\mathbf{y}_m=\sqrt{\frac{2E_s}{T_s}}\sum_{u=0}^{U-1}\mathbf{h}_{m,u(0)}\mathbf{s}_{u(0)}+\mathbf{i}_m+\mathbf{n}_m\,, \tag{3}$$

where E_s and T_s are respectively the symbol energy and the symbol duration. $\mathbf{s}_{u(0)}$ is the $N_c\times 1$ transmitted signal vector of u-th user of c=0th cell. $\mathbf{i}_m$ and $\mathbf{n}_m$ are respectively the $N_c\times 1$ CCI vector and the $N_c\times 1$ noise vector at the m-th receive antenna. $\mathbf{h}_{m,u(0)}$ is the $N_c\times N_c$ channel impulse response matrix given as

$$\mathbf{h}_{m,u(0)}=\begin{bmatrix} h_{m,u(0)}^{(0)} & & & h_{m,u(0)}^{(L-1)} & & \\ \vdots & \ddots & & & \ddots & \\ h_{m,u(0)}^{(L-1)} & & h_{m,u(0)}^{(0)} & \mathbf{0} & & h_{m,u(0)}^{(L-1)} \\ & \ddots & & h_{m,u(0)}^{(0)} & & \\ & & h_{m,u(0)}^{(L-1)} & & \ddots & \\ \mathbf{0} & & & \ddots & & h_{m,u(0)}^{(0)} \end{bmatrix}. \tag{4}$$

The received signal block $\mathbf{y}_m$ is transformed by N_c-point fast Fourier transform (FFT) into the frequency-domain signal. The frequency-domain signal vector $\mathbf{Y}_m=\left[Y_m(0)\ \cdots\ Y_m(N_c-1)\right]^T$ is expressed as [9]

$$\begin{aligned}\mathbf{Y}_m&=\mathbf{F}\mathbf{y}_m\\&=\sqrt{\frac{2E_s}{T_s}}\sum_{u=0}^{U-1}\mathbf{F}\mathbf{h}_{m,u(0)}\mathbf{F}^H\mathbf{F}\mathbf{s}_{u(0)}+\mathbf{F}\mathbf{i}_m+\mathbf{F}\mathbf{n}_m\\&=\sqrt{\frac{2E_s}{T_s}}\sum_{u=0}^{U-1}\mathbf{H}_{m,u(0)}\mathbf{F}\mathbf{s}_{u(0)}+\mathbf{I}_m+\mathbf{N}_m\\&=\sqrt{\frac{2E_s}{T_s}}\sum_{u=0}^{U-1}\overline{\mathbf{H}}_{m,u(0)}\mathbf{s}_{u(0)}+\mathbf{I}_m+\mathbf{N}_m\end{aligned}, \tag{5}$$

where $\mathbf{F}$ is the $N_c\times N_c$ FFT matrix and $\mathbf{H}_{m,u(0)}$ is the $N_c\times N_c$ diagonal matrix, given by

$$\begin{aligned}\mathbf{H}_{m,u(0)}&=\mathbf{F}\mathbf{h}_{m,u(0)}\mathbf{F}^H\\&=diag\left[H_{m,u(0)}(0),\ldots,H_{m,u(0)}(N_c-1)\right]\end{aligned} \tag{6}$$

where

$$H_{m,u(0)}(k)=\sum_{l=0}^{L-1}h_{m,u(0)}^{(l)}\exp(-j2\pi k\tau_l/N_c) \tag{7}$$

with $(.)^H$ representing the Hermitian transpose operation. In Eq. (5), $\overline{\mathbf{H}}_{m,u(0)}=\mathbf{H}_{m,u(0)}\mathbf{F}$, $\mathbf{I}_m$, and $\mathbf{N}_m$

are the equivalent channel matrix, the frequency-domain CCI vector, and the frequency-domain noise vector, respectively. By the use of expanded vector and matrix, all elements of N_r received signal can be expressed as

$$\begin{aligned}\mathbf{Y} &= \left[\mathbf{Y}_0 \quad \cdots \quad \mathbf{Y}_{N_r-1}\right]^T \\ &= \sqrt{\frac{2E_s}{T_s}}\begin{bmatrix} \overline{\mathbf{H}}_{0,0(0)} & \cdots & \overline{\mathbf{H}}_{0,U-1(0)} \\ \vdots & \ddots & \vdots \\ \overline{\mathbf{H}}_{N_r-1,0(0)} & \cdots & \overline{\mathbf{H}}_{N_r-1,U-1(0)} \end{bmatrix}\begin{bmatrix} \mathbf{s}_{0(0)} \\ \vdots \\ \mathbf{s}_{U-1(0)} \end{bmatrix} \\ &\quad + \begin{bmatrix} \mathbf{I}_0 \\ \vdots \\ \mathbf{I}_{N_r-1} \end{bmatrix} + \begin{bmatrix} \mathbf{N}_0 \\ \vdots \\ \mathbf{N}_{N_r-1} \end{bmatrix} \\ &= \sqrt{\frac{2E_s}{T_s}}\overline{\mathbf{H}}_{(0)}\mathbf{s}_{(0)} + \mathbf{I} + \mathbf{N}\end{aligned}, \quad (8)$$

where $\overline{\mathbf{H}}_{(0)}$, $\mathbf{s}_{(0)}$, $\mathbf{I}$, and $\mathbf{N}$ are the $N_rN_c \times UN_c$ expanded equivalent channel matrix, $UN_c \times 1$ expanded transmit signal vector, $N_rN_c \times 1$ expanded frequency-domain CCI vector, and $N_rN_c \times 1$ expanded frequency-domain noise vector, respectively. In this paper, we apply QRM-MLD to the expanded vector $\mathbf{Y}$. The detail of QRM-MLD is described in the next section.

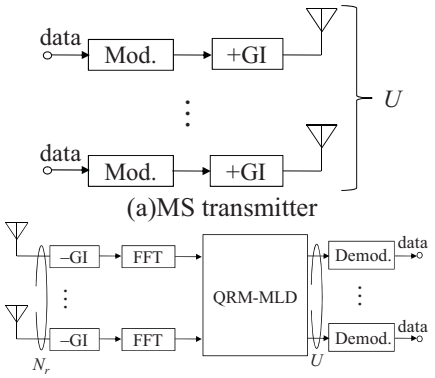

(a)MS transmitter

(b)BS receiver

Figure 2 Transmission system model of SC multi-user MIMO.

4 QRM-MLD

QR decomposition is applied to transform the expanded equivalent channel matrix $\overline{\mathbf{H}}_{(0)}$ into the upper triangle matrix $\mathbf{R}$ as

$$\overline{\mathbf{H}}_{(0)} = \mathbf{QR}, \quad (9)$$

where $\mathbf{Q}$ is an $N_rN_c \times UN_c$ matrix satisfying $\mathbf{Q}^H\mathbf{Q} = \mathbf{I}_{UN_c}$ ($\mathbf{I}_{UN_c}$ is the $UN_c \times UN_c$ identity matrix) and $\mathbf{R}$ is an $UN_c \times UN_c$ upper triangular matrix given as

$$\mathbf{R} = \begin{bmatrix} R_{0,0} & R_{0,1} & \cdots & R_{0,UN_c-1} \\ & R_{1,1} & \cdots & R_{1,UN_c-1} \\ & & \ddots & \vdots \\ & & & R_{UN_c-1,UN_c-1} \end{bmatrix}. \quad (10)$$

In this paper, we use the *sorted QR decomposition*, proposed in [10], as ordering. Then, the expanded received signal vector $\mathbf{Y}$ is transformed into $\hat{\mathbf{Y}} = \left[\hat{\mathbf{Y}}_0 \quad \cdots \quad \hat{\mathbf{Y}}_{U-1}\right]^T$ as

$$\begin{aligned}\hat{\mathbf{Y}} &= \mathbf{Q}^H\mathbf{Y} \\ &= \sqrt{\frac{2E_s}{T_s}}\begin{bmatrix} R_{0,0} & \cdots & R_{0,UN_c-1} \\ & \ddots & \vdots \\ \mathbf{0} & & R_{UN_c-1,UN_c-1} \end{bmatrix}\begin{bmatrix} s_0(0) \\ \vdots \\ s_{U-1}(N_c-1) \end{bmatrix} \\ &\quad + \mathbf{Q}^H\mathbf{I} + \mathbf{Q}^H\mathbf{N}\end{aligned}. \quad (11)$$

The M algorithm, which consists of UN_c stages, is applied to the vector $\hat{\mathbf{Y}}$. In each stage, the accumulated path metric based on squared Euclidian distance between $\hat{\mathbf{Y}}$ and each path arriving at the symbol candidates is calculated, and M symbol candidates having smallest accumulated path metric are selected as surviving symbol candidates. At the UN_c-th stage (which is the final stage), the best symbol candidate having the smallest accumulated path metric is chosen. The path arriving at the best symbol candidate is traced back to output the detected symbol block.

5 Computer simulation

Table 1 shows the simulation condition. The channel is assumed to be a frequency-selective block Rayleigh fading having a symbol-spaced L-path uniform power delay profile (i.e., $E\left[\left|g_{m,u(c)}^{(l)}\right|^2\right] = 1/L$). The transmit power $P=E_s/T_s$ is set so that the average received bit energy-to-noise power spectrum density ratio E_b/N_0 from a user at the cell edge is equal to 10 dB.

First, U users' locations are randomly generated in each cell for the given cluster size N. Next, the path-loss and the log-normally distributed shadowing loss are generated for each user. Then, an L-path block Rayleigh fading associated with each user is generated and signal transmission is simulated to measure the local average BERs of U users in the c=0th cell. This BER measurement is repeated a sufficient number of times by randomly changing the user locations to obtain the complementary cumulative distribution function (CCDF) of the local average BER.

The outage probability is defined as the probability that the local average BER exceeds the required BER. If the outage probability is less than the allowable outage probability Q, the number U of users is incremented by one. We define the cellular capacity as the maximum number $U_{\max}$ of supportable users normalized by the cluster size N. In this paper, we set the required BER and the allowable outage probability to BER=10^{-3} and Q=0.1, respectively. As a comparison, we also simulated the SC multi-user MIMO uplink signal transmission using MMSED and also computed the matched filter (MF) bound.

Table 1. Simulation condition

Transmitter	Data modulation	QPSK
	Number of users per cell	U=1~N_r
	Block size	N_c=64
	GI length	N_g=16
Channel	Fading type	Frequency-selective block Rayleigh
	Power delay profile	L=16-path uniform
	Path-loss exponent	α =3.5
	Standard deviation of shadowing loss	σ =7.0 dB
	Average received E_b/N_0 from cell edge	10 dB
Receiver	Number of receive antennas	N_r=4, 8
	Channel estimation	Ideal
Required quality	Required BER	10^{-3}
	Allowable outage probability	Q=0.1

Figure 3 illustrates the outage probability as a function of the number of users U, when N_r=4 and N=25. For MMSED, the outage probability significantly increases with U. This is because its diversity order is N_r–U+1 and decreases as U increases. By contrast, QRM-MLD can achieve lower outage probability than MMSED since its diversity order is N_r. Now, we focus on the case of M=1. In the case of U=N_r and M=1, the outage probability of QRM-MLD significantly increases. If U is lower than N_r, the receive antenna diversity effect can be obtained and therefore, lower outage probability is achieved even though only one symbol candidate is selected in each stage of the M algorithm. In the case of U=N_r, however, the receive antenna diversity effect cannot be achieved and the diagonal elements, especially R_{UN_c-1,UN_c-1}, of **R** become small. Therefore, the probability of discarding the correct symbol candidate increases and a large M must be used in the case of U=N_r.

Figure 4 shows the uplink capacity, $U_{\max}/N$, as a function of the cluster size N. The value of $U_{\max}$ is also indicated near each mark plotted in the figure. When N is small (i.e., up to N=9), the CCI power is too strong, and therefore, the difference of $U_{\max}$ between MMSED and QRM-MLD is at most 1 user only. As N increases, the CCI power gets weaker and therefore, more users can be accommodated in one base station. However, even though N increases (i.e., CCI power decreases), the uplink capacity of MMSED does not increase and are less than that of N=9 case. This is because the diversity order of MMSED is equal to N_r–U+1, and hence, increasing the value of N does not improve the uplink capacity. On the other hand, for QRM-MLD, the maximum uplink capacity gets larger than the capacity of N=9 case since QRM-MLD can obtain the diversity order of N_r.

Then, we discuss the relation between the maximum uplink capacity and the computational complexity. Figure 5 shows the maximum uplink capacity of QRM-MLD as a function of the number of surviving symbol candidates M. The value of N is also indicated near each mark plotted in the figure. The complexity is measured as the number of complex multiply operations. The numbers of multiply operations of both QRM-MLD and MMSED are shown in table 2 and 3. In table 2, X denotes the modulation level.

In the case of N_r=4, QRM-MLD can obtain about 1.7 times (2.3 times) larger maximum capacity compared to MMSED at the cost of about 5.2 × 10^3 times (6.9 × 10^3 times) larger complexity for M=1 (M=64). Similarly, in the case of N_r=8, QRM-MLD can obtain about 1.6 times (1.8 times) larger maximum capacity compared to MMSED at the cost of 9.3 × 10^3 times (1.4 × 10^4 times) larger complexity for M=1 (M=64). It can be seen that the effect of QRM-MLD upon the increase of the uplink capacity compared to MMSED relatively decreases as the number of receive antennas increases. This is because as the number of receive antennas increases from 4 to 8, the number of users, at the value of N which maximizes the uplink capacity, increases by 3 times for MMSED and by 2.3 times (2.7 times) for QRM-MLD when M=1 (M=64).

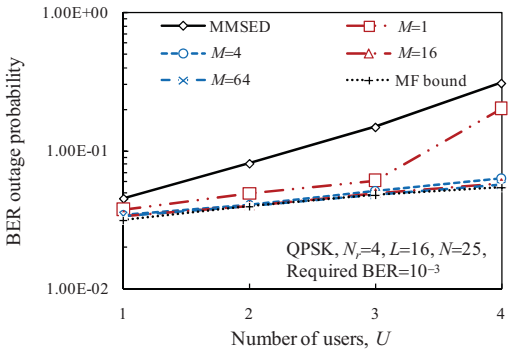

Figure 3 Outage probability comparison.

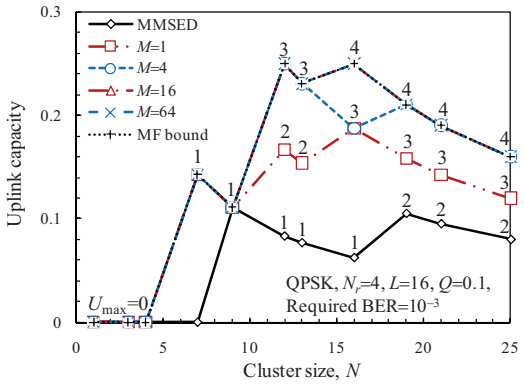

(a)N_r=4.

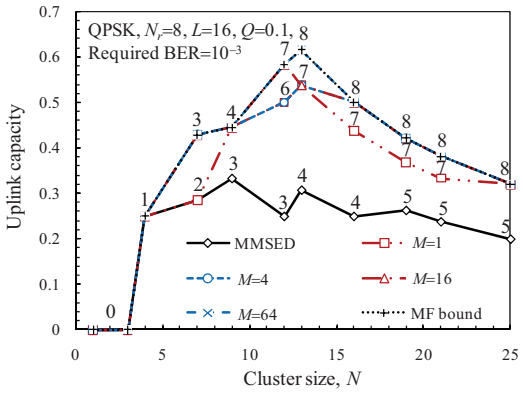

(b)N_r=8

Figure 4 Uplink capacity.

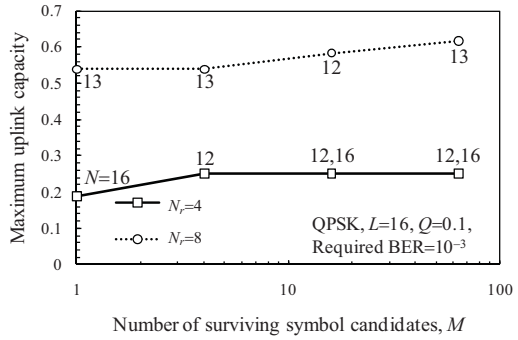

Figure 5 Maximum uplink capacity of QRM-MLD.

Table 2. Number of complex multiple operations of QRM-MLD

	No. of complex multiplications
FFT	$N_rN_c\log_2N_c$
Calculation of equivalent channel matrix	$N_rUN_cL+N_rUN_c^2$
Sorted QR decomposition [10]	$(1/2)UN_rN_c^2(3UN_c-1)$
Multiplication of $\mathbf{Q}^H$	$N_rUN_c^2$
Calculation of squared Euclidian distance	$X\{2+(M/2)(UN_c+4)(UN_c-1)\}$

Table 3. Number of complex multiple operations of MMSED

	No. of complex multiplications
FFT	$N_rN_c\log_2N_c$
Signal detection	$N_c\{U^3+2N_rU^2+N_rU\}$
IFFT	$UN_c\log_2N_c$

6 Conclusions

In this paper, we introduced frequency domain QRM-MLD block signal detection into the uplink broadband SC multi-user MIMO in a cellular system and examined how it can enhance the uplink capacity compared to MMSED. For MMSED, increasing the value of N does not improve the uplink capacity since its diversity order decreases as U. On the other hand, QRM-MLD can achieve the diversity order of N_r and therefore, larger uplink capacity is obtained. We showed that QRM-MLD block signal detection can obtain about 2.3 times larger uplink capacity at the cost of about 6.9 × 10^3 times higher complexity when N_r=4 and M=64.

References

[1] Q. H. Spencer, C. B. Peel, A. L. Swindlehurst, and M. Haardt, "An introduction to the multi-user MIMO downlink," IEEE Commun. Mag., Vol. 42, No. 10, pp.60-67, Oct. 2004.

[2] S. Sfar, R. D. Murch, and K. B. Letaief, "Layered space-time multiuser detection over wireless uplink systems," IEEE Trans. Wireless Commun., Vol. 2, No. 4, pp.653-668, July 2003.

[3] J. G. Proakis, *Digital communications*, 4th edition, McGraw-Hill, 2001.

[4] W. C. Jakes, Jr., ed., *Microwave mobile communications*, John Wiley & Sons, New York, 1974.

[5] T. Chiba, K. Takeda, and F. Adachi, "Uplink capacity of a single-carrier multi-user MIMO multiplexing in a frequency-selective channel," The 11th WPMC, Sep. 8-11, 2008.

[6] L. J. Kim, and J. Yue, "Joint channel estimation and data detection algorithms for MIMO-OFDM systems," in Proc. 36thThirty-Sixth Asilomar Conference on Signals, System and Computers, pp. 1857-1861, Nov. 2002.

[7] S. Sun, Y. Dai, Z. Lei, K. Higuchi, and H. Kawai, "Pseudo-inverse MMSE based QRD-M algorithm for MIMO-OFDM," The IEEE 63rd Vehicular Technology Conference (VTC-Spring), Melbourne, Australia, May, 2006.

[8] T. Yamamoto, K. Takeda, and F. Adachi, "Single-carrier transmission using QRM-MLD with antenna diversity," The 12th WPMC, 7-10 Sep. 2009.

[9] T. Yamamoto, K. Takeda, and F. Adachi, "A study of frequency-domain signal detection for single-carrier transmission," IEEE 70th Vehicular Technology Conference (VTC-Fall), 20-23 Sep. 2009.

[10] D. Wuebben, R. Boehnke, J. Rinas, V. Kuehn, and K. D. Kammeyer, "Efficient algorithm for decoding layered space-time codes," IEE Electronics Letters, Vol. 37, no. 22, pp. 1348-1350, Oct. 2001.